TISSUE ENGINEERING: Part C
Volume 20, Number 2, 2013
© Mary Ann Liebert, Inc.
DOI: 10.1089/ten.tec.2013.0176

Methods Article

A Facile Method to Fabricate Hydrogels with Microchannel-Like Porosity for Tissue Engineering

Joshua Hammer, BSc,[1,*] Li-Hsin Han, PhD,[2,*] Xinming Tong, PhD,[2] and Fan Yang, PhD[2,3]

Hydrogels are widely used as three-dimensional (3D) tissue engineering scaffolds due to their tissue-like water content, as well as their tunable physical and chemical properties. Hydrogel-based scaffolds are generally associated with nanoscale porosity, whereas macroporosity is highly desirable to facilitate nutrient transfer, vascularization, cell proliferation and matrix deposition. Diverse techniques have been developed for introducing macroporosity into hydrogel-based scaffolds. However, most of these methods involve harsh fabrication conditions that are not cell friendly, result in spherical pore structure, and are not amenable for dynamic pore formation. Human tissues contain abundant microchannel-like structures, such as microvascular network and nerve bundles, yet fabricating hydrogels containing microchannel-like pore structures remains a great challenge. To overcome these limitations, here we aim to develop a facile, cell-friendly method for engineering hydrogels with microchannel-like porosity using stimuli-responsive microfibers as porogens. Microfibers with sizes ranging 150–200 μm were fabricated using a coaxial flow of alginate and calcium chloride solution. Microfibers containing human embryonic kidney (HEK) cells were encapsulated within a 3D gelatin hydrogel, and then exposed to ethylenediaminetetraacetic acid (EDTA) solution at varying doses and duration. Scanning electron microscopy confirmed effective dissolution of alginate microfibers after EDTA treatment, leaving well-defined, interconnected microchannel structures within the 3D hydrogels. Upon release from the alginate fibers, HEK cells showed high viability and enhanced colony formation along the luminal surfaces of the microchannels. In contrast, HEK cells in non-EDTA treated control exhibited isolated cells, which remained entrapped in alginate microfibers. Together, our results showed a facile, cell-friendly process for dynamic microchannel formation within hydrogels, which may simultaneously release cells in 3D hydrogels in a spatiotemporally controlled manner. This platform may be adapted to include other cell-friendly stimuli for porogen removal, such as Matrix metalloproteinase-sensitive peptides or photodegradable gels. While we used HEK cells in this study as proof of principle, the concept described in this study may also be used for releasing clinically relevant cell types, such as smooth muscle and endothelial cells that are useful for repairing tissues involving tubular structures.

Introduction

Hydrogels are widely used as three-dimensional (3D) scaffolds for tissue engineering due to their tissue-like water content and ease of cell encapsulation, as well as their tunable physical and chemical properties.[1–7] Many hydrogel-based scaffolds are in lack of cell-size pores (macropores), whereas macroporosity is highly desirable to facilitate cell migration, proliferation, extracellular matrix (ECM) deposition, and faster blood vessel in-growth.[8–13] Given the importance of macroporosity to promote desirable tissue regeneration, diverse technologies have been developed to fabricate 3D macroporous scaffolds for tissue engineering, including electrospinning,[14,15] lyophilization,[16,17] gas foaming,[18] stereolithography,[19–21] micromolding,[22,23] porogen leaching,[24–27] and laser sintering.[28] These methods generally result in the formation of spherical macropores, yet fabricating hydrogels containing microchannel-like pore structures remains a great challenge. Human tissues contain abundant microchannel-like structures, such as microvascular network and nerve bundles.[29,30] These channels serve important functions to deliver nutrients and oxygen, remove metabolic waste, conduct neuronal signals, and are critical for regenerating tissues with clinical relevant dimensions.[31,32] Furthermore, such microchannel structures may also provide topographical cues to guide cell arrangement to form blood vessels[33] and nerve bundles.[34]

Recent efforts to create microchannels in 3D scaffolds have employed techniques, such as modular assembly of submillimeter-sized collagen gel rods, 3D bioprinting, layer-by-layer assembly, microfluidics, and use of cell-degradable

[1]School of Biological and Health Systems Engineering, Arizona State University, Tempe, Arizona.
Departments of [2]Orthopaedic Surgery and [3]Bioengineering, Stanford University, Stanford, California.
*These authors contributed equally to this work.

or sacrificial template.[13,33,35–40] These methods are often slow and involve complex processes, and are difficult to apply to engineer large tissues needed for repairing critical-size defects. Furthermore, most methods involve fabrication conditions that are not cell-friendly, such as the use of organic solvents, high temperature and nonphysiological salt-concentrations.[24,25,41] Moreover, current techniques are mainly designed for creating hydrogels with fixed microchannel structure, and do not accommodate dynamic microchannel formation in a temporally-controlled manner. While low porosity may be preferable during initial stages to protect transplanted cells, increased microchannel formation overtime would be desirable to provide space for cell proliferation and new matrix formation.

To overcome the above limitations, here we report a facile, cell-friendly process to fabricate hydrogels with microchannel-like porosity using stimuli-responsive microfibers. These microfibers not only facilitate dynamic formation of microchannel-like pore structures, but also allow release of cells within 3D hydrogels in a stimuli-responsive manner. Specifically, calcium alginate (Ca-Alg)-based microfibers were encapsulated within photocrosslinkable hydrogels composed of methacrylated gelatin (Gel-MA). To form microchannels in Gel-MA scaffolds, the Ca-Alg microfibers were dissolved using ethylenediaminetetraacetic acid (EDTA), a calcium chelator, leaving behind cylindrical lumen spaces (Fig. 1C, D). By encapsulating cells within the microfibers, the Ca-Alg microfibers also served as effective cell delivery vehicles, which released the cells to spread on the lumen walls (Fig. 1A, B). Compared with the previously reported methods for microchannel formation,[13,33,35–40] our method is fast and facile, allows dynamic formation of microchannels, and may be used to release cells in a spatiotemporally controlled manner within 3D hydrogels. To examine the effect of microchannel formation on cell viability and distribution, human embryonic kidney cells (HEKs) were encapsulated within Ca-Alg microfibers before being encapsulated within a Gel-MA scaffold. Scanning electron microscopy was used to analyze macropore morphology. The effect of EDTA exposure on cell-containing Ca-Alg microfibers and cell morphology were examined using live-dead staining and confocal microscopy at multiple time points.

Materials and Methods

Materials

Gelatin (types A and B), glycidyl methacrylate, sodium alginate salt, dimethyl phenylphosphonite, 2,4,6-trimethylbenzoyl chloride, lithium bromide, 2-butanone, and perfluorinated oil FC-70 were purchased from Sigma-Aldrich. Disodium citrate (DSC), EDTA, sodium chloride, and calcium chloride dehydrate were purchased from Fisher Scientific.

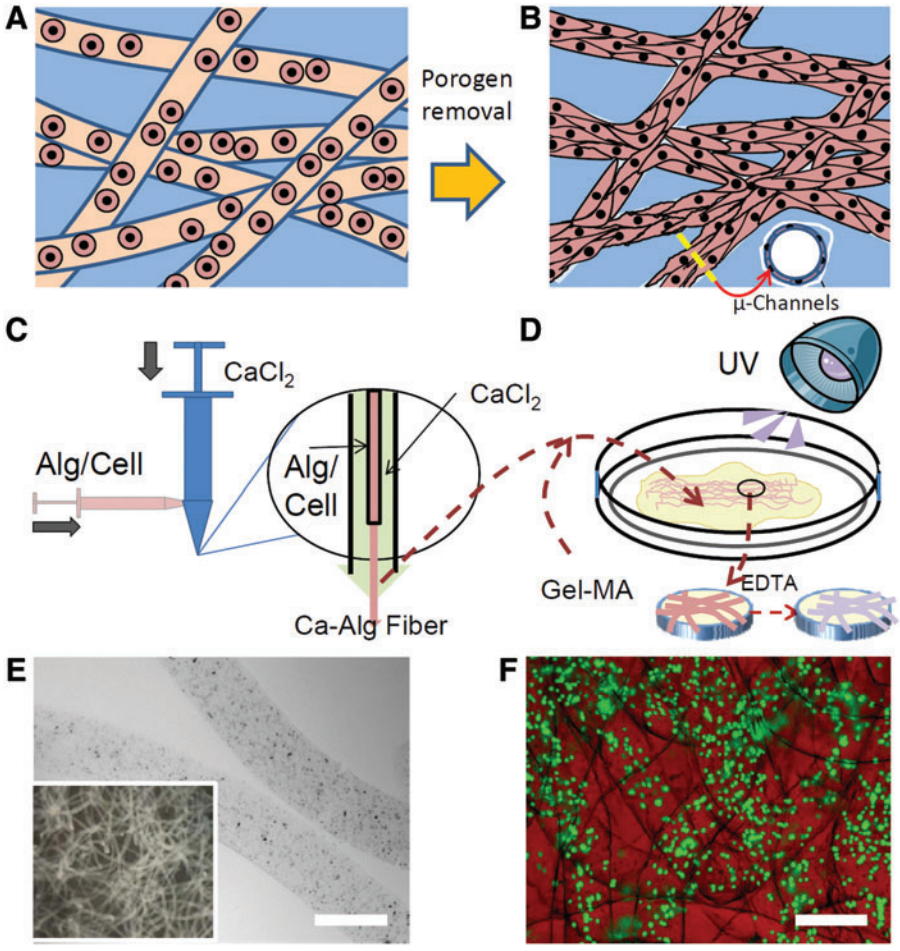

FIG. 1. Experimental scheme for dynamic microchannel formation. **(A, B)** Releasing cells from microfibers; **(C)** fabricating calcium alginate (Ca-Alg) microfibers with a coaxial needle set; **(D)** encapsulating Ca-Alg microfibers in gelatin hydrogel and dissolving the microfibers by ethylenediaminetetraacetic acid (EDTA); **(E)** Ca-Alg microfibers under optical microscope; The inset shows the morphology of a network-like bundle of microfiber Ca-Alg microfibers. **(F)** Ca-Alg microfibers with human embryonic kidney (HEK) cells under fluorescent microscope. Scale bars for **(E, F)** 200 μm. Color images available online at www.liebertpub.com/tec

Precursors for microfibers and hydrogels

The following methods are partially used in our previous study about spherical-macropore formation.[42] Sodium alginate, previously purified by dialysis then lyophilized, was dissolved at 2% (w/v) in Dulbecco's modified Eagle's medium (DMEM). Calcium chloride solution ($CaCl_2$) was prepared by dissolving 1% (w/v) calcium chloride and 0.9% (w/v) sodium chloride in water. Methacrylated gelatin (Gel-MA) was synthesized as previously reported[35] using type-B gelatin (GelB), the alkali-denatured collagen that presents collagen-based binding cell sites in our hydrogel. In brief, GelB (10 g) was dissolved in 100 mL dulbecco's phosphate-buffered saline (DPBS) under 50°C, and methacrylic anhydride (20 mL) was slowly added under constant stirring at 1000 rpm. The reaction continued for 3 h at 50°C. Crude product of Gel-MA was extracted by dripping the solution into acetone (3L), which precipitated Gel-MA and removed excessive methacrylic anhydride and by products. The Gel-MA was purified by dialysis in DI water, lyophilized, and stored at −20°C until use. Photoinitiator lithium phenyl-2,4,6-trimethylbenzoylphosphinate (LAP) was prepared according to existing protocol.[43] In brief, at room temperature and under argon, 2,4,6-trimethylbenzoyl chloride (3.2 g) was added dropwise to continuously stirred dimethylphenylphosphonite (3.0 g), and the mixture was stirred for 18 h, whereupon the reaction mixture was heated to 50°C, and excess of lithium bromide (6.1 g) in 2-butanone (100 mL) was added to the mixture. After 10 min, the mixture was cooled to ambient temperature, allowed to rest for 4 h and filtered to collect precipitate. The filtrate was washed and filtered three times with 2-butanone to remove unreacted lithium bromide, and excess solvent was removed by vacuum. To prepare hydrogel precursor, Gel-MA was dissolved at 10% (w/v) with 0.05% LAP photoinitiator in phosphate-buffered saline (PBS). Type-A gelatin (GelA) was purified through dialysis then lyophilized before being dissolved at 10% (w/v) in 45°C PBS. EDTA solution was prepared at either 8 mM with 12 mM DSC or 16 mM EDTA with 24 mM DSC in DMEM. All solutions were prepared under sterile conditions.

Fabricating stimuli-responsive Ca-Alg microfibers

Ca-Alg microfibers were spun with a coaxial needle set that took advantage of shear stress generated by unequal fluid velocities between coaxial flow layers.[44] To fabricate the coaxial needle set, a 30G "core" needle was located coaxially in a 22G "sheath" needle, and inlets were built to guide separate fluids through the core and sheath needles. The needle set was fixed using acrylic resin (Fig. 1C). More details of the coaxial needle set are shown by Supplementary Figure S1 in the Supplementary Materials (Supplementary Materials are available online at www.liebertpub.com/tec). To spin microfibers, sodium alginate solution was pumped through the core needle at 3.0 mL/min, while $CaCl_2$ was pumped through the sheath needle at 48 mL/min. As the flows merged in the coaxial channel, Ca^{2+} from the sheath flow crosslinked the alginate core flow to form Ca-Alg microfibers (diameter: 100- 200 μm). Fibers were collected in a cell strainer and exposed to a reservoir of $CaCl_2$ solution for 3 min before being transferred to DMEM containing 10% fetal bovine serum and 1% penicillin streptomycin (complete DMEM), and incubated at 37°C and 5% CO_2 overnight.

Encapsulating Ca-Alg microfibers in hydrogel scaffold

To assist microchannel formation, before encapsulation the Ca-Alg microfibers made from 2 mL sodium alginate solution were soaked in GelA solution (5 mL) at 37°C for 3 min, which forms a gelatin coating on the microfibers that prevents the diffusion of Gel-MA precursor into the microfibers. The coated microfibers were transferred to a cell strainer and were rinsed three times by warm (37°C) Gel-MA solution (200 μL each time) to remove excess GelA. To form a hydrogel, the amount of Gel-MA precursor was adjusted to make the final volume of the Gel-MA/microfiber mixture equal to 1.0 mL, and the mixture was transferred to multiple cylindrical moldings (5.6 mm in diameter and 3 mm in thickness). To crosslink the Gel-MA precursor, the moldings with Gel-MA/microfiber mixture were exposed to light (4 min, 365 nm at 2.5 mW/cm^2), which turned the precursor into cylindrical hydrogels. The hydrogel with Ca-Alg microfibers was collected from the molding and incubated at 37°C and 5% CO_2 in PBS for 24 h before further treatments.

Dynamic microchannel formation

Microchannel formation. To induce microchannel formation, the Gel-MA hydrogels with microfibers were incubated in EDTA solution (16 mM EDTA + 24 mM DSC in DMEM) for 2 h. The treated hydrogels were rinsed by PBS and placed back into incubation. The effect of microchannel formation was studied 2 h and 2 days after the EDTA treatment.

Characterizing pore morphology. To study the efficacy of dynamic microchannel formation, variable pressure scanning electron microscopy (VP-SEM, Hitachi S-3400N) was used to monitor the changes in internal structure of hydrogel samples following EDTA treatment (on day 0 and 2). The hydrogels were cut using a razor to expose the cross-sections, and loaded into the VP-SEM chamber where they were gradually cooled from ambient temperature to −20°C, while the chamber pressure was reduced from atmospheric pressure to 50 Pa following a liquid water P/T curve. SEM images were acquired under 15 kV electron beam at ~7 mm working distance.

Stimuli-responsive microfibers as a cell delivery mechanism

Cell encapsulation and delivery using stimuli-responsive microfibers. Trypsinized HEK cells were suspended in sodium alginate solution (5 million/mL), and the cell-laden alginate solution (2 mL) was spun into Ca-Alg microfibers following the aforementioned procedures (Fig. 1E, F). The microfibers were incubated for 24 h in HEK culture medium containing high glucose DMEM, 10% (v/v) fetal bovine serum, 100 U/mL penicillin, and 0.1 mg/mL streptomycin. After 24 h incubation, cell-laden Ca-Alg microfibers were encapsulated in Gel-MA scaffold following the aforementioned steps. However, to facilitate fluorescence imaging, in which thinner samples are preferred, the Gel-MA/microfiber mixture with cells was molded using a Teflon plate, a Petri-dish and a 500 μm-thick spacer, which shaped the mixture into a hydrogel sheet (500 μm-thick) upon exposure to UV light (Fig. 1D). To enhance the release of the hydrogel sheet, the Teflon plate was precoated with a thin layer of

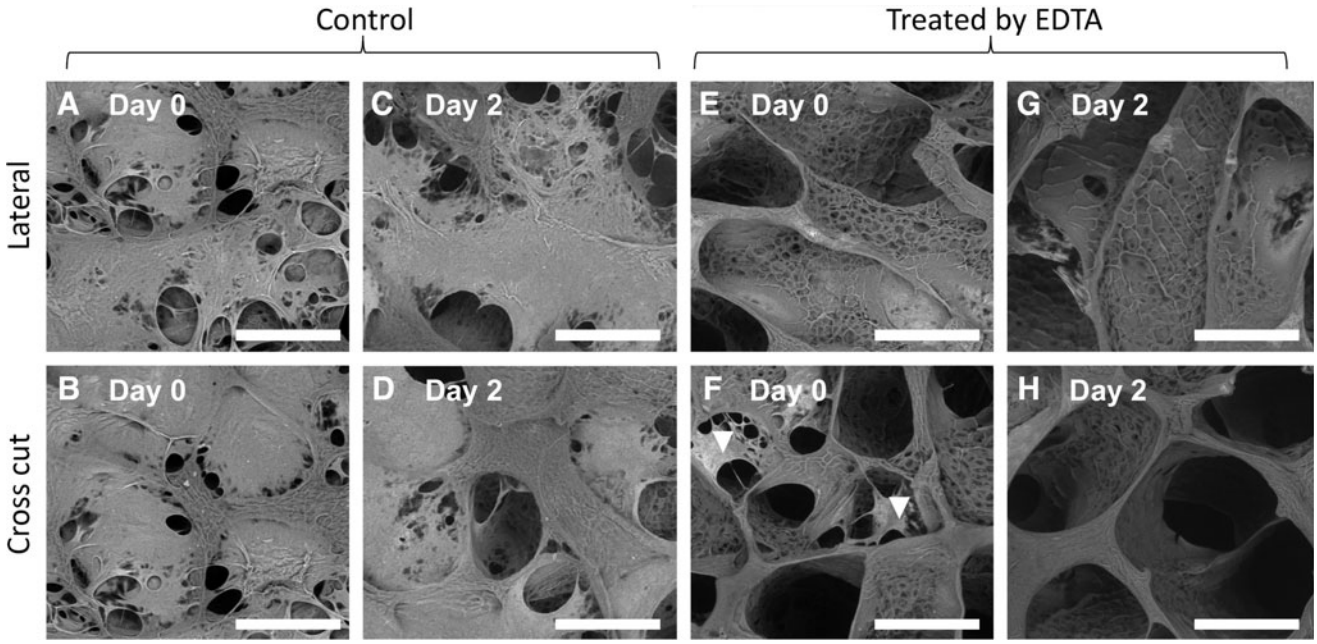

FIG. 2. Changes of microfiber-containing hydrogel morphology by scanning electron microscopy on day 0 and 2. **(A–D)** Untreated control showed negligible change in scaffold morphology from day 0 to 2; **(E–H)** Experimental group treated by EDTA (16 mM EDTA) exhibited dissolution of Ca-Alg microfiber and complete formation of microchannels within hydrogels over 2 days. Scale bars: 200 μm.

fluorinated oil FC-70. The hydrogel sheet was cut using a polypropylene straw into smaller samples (~8 mm in diameter) and the samples were incubated in HEK culture medium in a standard 48-well plate for 24 h before EDTA treatments. To dissolve Ca-Alg microfibers and simultaneously release HEK cells into microchannels, the Gel-MA hydrogels were rinsed by serum-free DMEM and were exposed to EDTA at various concentrations (8 mM EDTA + 12 mM DSC or 16 mM EDTA + 24 mM DSC) for different durations (1 or 2 h). To remove EDTA residue, the treated samples were rinsed five times with culture medium (5 min each time).

Quantifying cell viability, morphology, and colony area. On days 1, 3, and 5, hydrogel samples from different groups (different EDTA treatments) were collected for Live/Dead and Hoechst staining (Invitrogen) following manufacture's protocols, and fluorescence images were taken with a Zeiss microscope. On the same days, the proliferation of cells in each hydrogel sample was quantified using WST-8 assays (Cayman Chemical) following manufacture's protocols (as shown by Supplementary Fig. S2 in the Supplementary Materials). On day 5, hydrogels were fixed in 4% paraformaldehyde for 2 h and stored in PBS at 4°C until processed. Fixed hydrogels were then stained by fluorescein phalloidin (Sigma-Aldrich) and Hoechst staining, and cell distribution in 3D was examined using a confocal microscope (Lesica SP5; Leisica Microsystems). Cell colony areas were quantified by analyzing the Live/Dead images using the open-source program ImageJ.

Statistical analysis

All data were expressed as mean ± standard error and statistical significance was determined by analysis of variance using student's t-test with equal variance. *p*-values (two-tails) of less than 0.05 were considered statistically significant, and *p*-values less than 0.005 were considered statistically highly significant.

Results

Microchannel formation using stimuli-responsive microfibers

The effectiveness of using stimuli-responsive microfibers for microchannel formation, as illustrated by Figure 1C and D, was examined using VP-SEM. On day 0, the control group (no exposure to EDTA) presented clear structures of Ca-Alg microfibers embedded within the Gel-MA hydrogel network (Fig. 2A, B). In contrast, EDTA-treated samples showed the formation of microchannels at the place where the Ca-Alg microfibers used to be (Fig. 2E, F). There were still some noticeable microfibers residues within the microchannels at day 0, suggesting that the diffusion of alginate out of the microchannels was not yet complete (Fig. 2F). By day 2, the EDTA-treated groups displayed a network of complete microchannel formation with no noticeable microfiber residues (Fig. 2G, H), while the Ca-Alg fibers remained intact in the control group (Fig. 2C, D).

Cell delivery using stimuli-responsive microfibers

To examine the efficacy of using Ca-Alg microfibers for cell delivery within hydrogels, hydrogels containing HEK-laden microfibers were exposed to EDTA at different doses (Fig. 3). Changes in cell morphology and viability in the hydrogels were monitored using Live/Dead staining in conjunction with nuclei staining (Hoechst) on days 1, 3, and 5 (Fig. 3). Cell distribution in 3D hydrogels was examined using confocal microscopy (Fig. 4). On day 1, the HEK cells

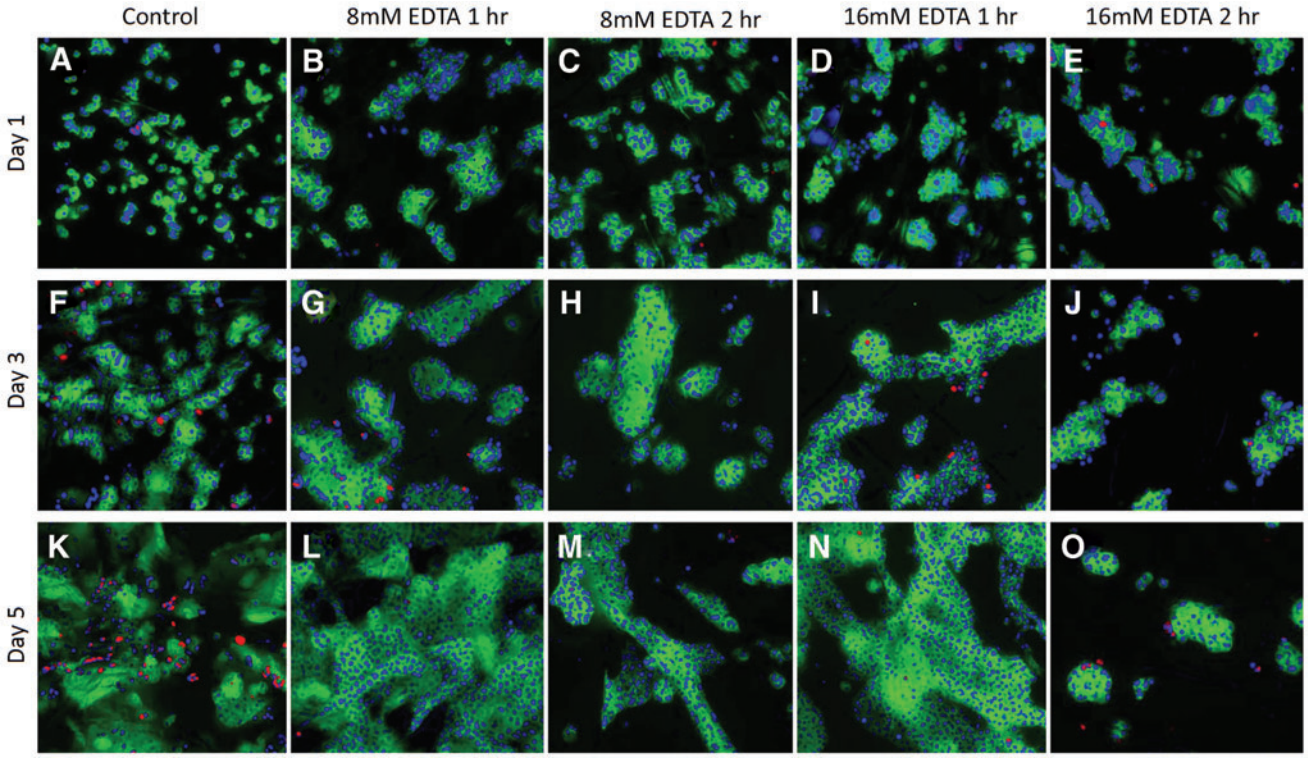

FIG. 3. Effects of EDTA exposure at varying doses on cell viability and morphology over 5 days. **(A, F, K)** Groups with no EDTA treatment showed small clusters remain entrapped in the intact Ca-Alg microfibers; groups treated with EDTA led to cell release and the formation of large cell colonies; **(B, G, L)** groups treated with 8 mM EDTA and 12 mM disodium citrate (DSC) for 1 h; **(C, H, M)** groups treated with 8 mM EDTA and 12 mM DSC for 2 h; **(D, I, N)** groups treated with 16 mM EDTA and 24 mM DSC for1 h; **(E, J, O)** Exposure to 16 mM EDTA and 24 mM DSC for 2 h. Color images available online at www.liebertpub.com/tec

in the EDTA-treated hydrogels were released from Ca-Alg fibers, spread and formed cell patches inside the lumens of the microchannels (Fig. 3B–E). Cells in the control group (nontreated) remained trapped in the Ca-Alg microfibers (Fig. 3A). By day 3, large colonies of HEK cells started to emerge in all groups treated by EDTA (Fig. 3G–J), whereas minimal cell clustering was observed in the control group (Fig. 3F). By day 5, the groups treated by EDTA showed extensive expansion of HEK colonies (Fig. 3L–O), whereas the HEK cells in the control groups increased in number but maintained small clusters in the Ca-Alg microfibers (Fig. 3K). The groups treated by EDTA presented high cell viability up

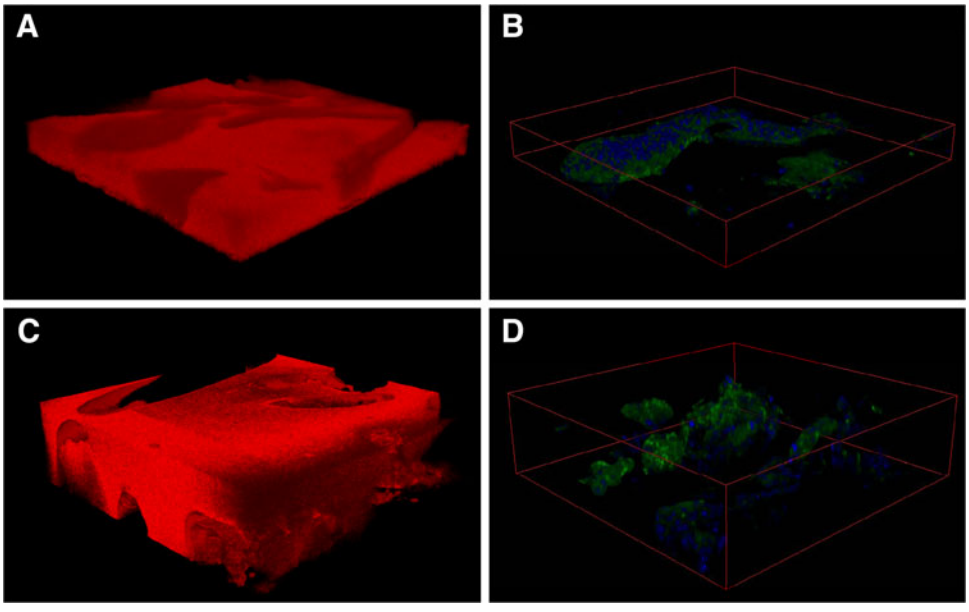

FIG. 4. Cell morphology within hydrogels on day 5, as shown by confocal microscopy. **(A, B)** The EDTA-treated group (16 mM EDTA + 24 mM DSC, 1 h) exhibited formation of large cell colonies along the wall of the microchannel; **(C, D)** The nontreated group exhibited isolated, small cell clusters entrapped in the intact microfiber. **(A)** and **(C)** show the three-dimensional morphology of microchannels; **(B)** and **(D)** show the distribution of HEK cells (blue: cell nuclei, green: cytoskeleton). Color images available online at www.liebertpub.com/tec

to day 5 (>95%). In contrast, the control group exhibited increased cell death over time (Fig 3A, F, K). Confocal imaging also shows that the EDTA treatment resulted in cell colony formation along the lumen wall of the microchannels (Fig. 4B), while cells remain entrapped in the microfibers in the control group (Fig. 4D).

Histogram analysis of area covered by cell colony shows that the groups exposed to 8 and 16 mM EDTA for a shorter time (1 h) presented the highest level of colony expansion, while the control group exhibited minimal colony formation (Fig. 5). Among the EDTA-treated groups, the group exposed to the highest dose of EDTA (16 mM, 2 h) presented the lowest level of colony expansion.

Discussion

Here we report a facile, cell-friendly process that allows dynamic formation of microchannels within bulk hydrogels using stimuli-responsive microfibers. We further showed such microfibers can be used for delivering cells within bulk hydrogels in a spatiotemporally-controlled manner. Exposure to a chemical stimulus, in this case EDTA, caused the dissolving of the Ca-Alg microfibers, leaving behind microchannel-like porosity within bulk hydrogels (Fig. 2). The microchannels created by microfiber removal are highly interconnected and the diameter of microchannels can be tuned by modulating the diameter of the microfibers. The resulting microchannels (150–200 μm in diameter) may promote tissue formation by facilitating vascularization, cell proliferation, and production of ECM components. Given that matrix topographical cue is one important factor for regulating tissue development, we speculate that the formation of microchannel structures within hydrogel scaffolds may facilitate engineering tissue that contain tubular structures such as microvasculature network or nerve bundles. By optimize other niche cues, such as growth factors and ECM components, the microchannel structures may promote more effective formation of such tubular tissues.

To examine the effects of dynamic microchannel formation on cell proliferation and morphology in 3D, we have chosen HEK 293 cells (HEK cells),[45] a commonly used cell type in cell biology as the model cell type and encapsulated HEKs in Ca-Alg microfibers, followed by embedding the microfibers in Gel-MA hydrogels. Exposures to EDTA induced the formation of mono-layered cell colonies along the lumen wall of microchannels (Figs. 3, 4B, and 5), while cells in the control group (no EDTA) remain entrapped in 3D Ca-Alg microfibers (Figs. 3, 4D, and 5). This is consistent with the results from SEM imaging (Fig. 2), which showed that the EDTA treatment led to well-defined lumen surfaces for cell adhesion, migration, and colony formation. While groups treated by EDTA showed consistent high cell viability, increasing cell death was observed from the untreated control, which may be caused by the limited nutrient diffusion for the cells entrapped in the microfibers. Higher doses of EDTA exposure (16 mM, 2 h) resulted in more cell death, accompanied by less cell colony formation by day 5. The higher dose of EDTA might have decreased cell viability and the level of colony formation by affecting the calcium-dependent cell membrane proteins that regulate cell-cell adhesion and cell proliferation, such as cadherin proteins. Together, our results show that low EDTA exposure (8 mM, 1 h) is sufficient for microchannel formation and subsequent cell delivery, and prolonged exposure to EDTA (>2 h) may cause significant cytotoxicity to HEKs.

Our results demonstrate several advantages of the platform developed herein in comparison with previously reported microchannel-forming methods. First, we demonstrate the potential of using stimuli-responsive microfibers to control cell distribution in 3D and release cells in a temporally controlled manner, which may be particularly useful for patterning cells into microtubular structures in 3D tissue engineering constructs. Several groups have recently demonstrated the use of sacrificial materials or cell-degradable templates to create channels within a bulk scaffold, such as shellac fibers,[46] collagen gel rods[13] and carbohydrate glass framework,[31] but these materials are not capable of controlled cell release and do not allow dynamic microchannel formation. Second, at optimal EDTA doses our process for microchannel formation did not result in noticeable changes in HEK cell viability and proliferation, as shown by live-dead staining and the quantitative WST assay, and allowed more homogeneous cell distribution in microchannels, which is important to mediate cell viability and tissue-forming efficiency in 3D.

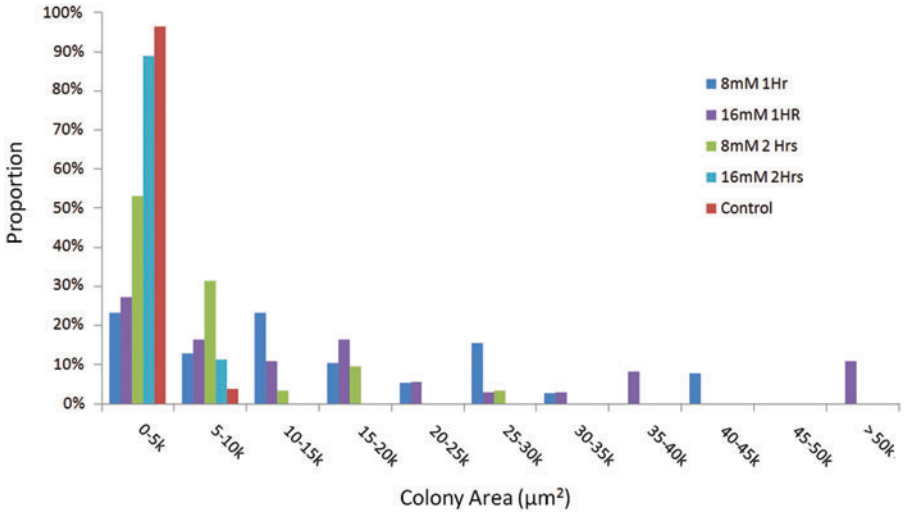

FIG. 5. Histogram of the area of cell colony distribution on day 5. Cell number from each group is greater than 300, and EDTA (8 and 16 mM) exposure for shorter period (1 h) resulted in the formation of larger cell colonies. Color images available online at www.liebertpub.com/tec

Using Ca-Alg as a model stimuli-responsive material, here we demonstrated the concept of dynamic microchannel-formation as well as the potential of controlling cell delivery in a temporal manner to facilitate tissue formation. This platform may be further extended by exploiting other materials as porogens that can be degraded using cell-friendly stimuli, such as hydrolysis, MMP-sensitive peptides[47] or photo-degradation.[48] While we used HEK cells as a model cell type to demonstrate the proof-of-principal in this study, the reported method of dynamic microchannel formation may also be applied for other cell types, such as smooth muscle cells and endothelial cells to engineer tubular tissues structures that are of clinical significance.

Conclusion

In summary, here we report a facile method to create microchannel-like structures within hydrogel scaffolds using alginate microfibers that can dissolve upon exposure to EDTA. Using optimized EDTA concentration and duration, this method also allows cell delivery in bulk hydrogels within the formed microchannel structures. Upon exposure to EDTA, a well-defined, interconnected microchannel network was created and cells were free to migrate and form colonies along the channels' internal surfaces, leading to laminar distribution of cells in 3D. The platform reported herein offers spatiotemporal control over cell seeding and distribution. Future iterations of this technique may lead to low-cost, sizable fabrication of engineered tissue grafts with enhanced cell viability and tissue formation efficiency, such as prevascularized tissue engineering building blocks.

Acknowledgments

The authors would like to thank the McCormick Faculty Award and Stanford Bio-X Interdisciplinary Initiative grant for funding. J.H. would like to acknowledge The Amgen Foundation for funding.

Disclosure Statement

This work has been disclosed to the Office of Technology Licensing at Stanford University.

References

1. Nguyen, K.T., and West, J.L. Photopolymerizable hydrogels for tissue engineering applications. Biomaterials **23,** 4307, 2002.
2. Langer, R., and Vacanti, J.P. Tissue engineering. Science **260,** 920, 1993.
3. Mosiewicz, K.A., Johnsson, K., and Lutolf, M.P. Phosphopantetheinyl transferase-catalyzed formation of bioactive hydrogels for tissue engineering. J Am Chem Soc **132,** 5972, 2010.
4. DeForest, C.A., Polizzotti, B.D., and Anseth, K.S. Sequential click reactions for synthesizing and patterning three-dimensional cell microenvironments. Nat Mater **8,** 659, 2009.
5. Flaim, C.J., Chien, S., and Bhatia, S.N. An extracellular matrix microarray for probing cellular differentiation. Nat Methods **2,** 119, 2005.
6. Chan, A.W., and Neufeld, R.J. Modeling the controllable pH-responsive swelling and pore size of networked alginate based biomaterials. Biomaterials **30,** 6119, 2009.
7. Chan, A.W., and Neufeld, R.J. Tuneable semi-synthetic network alginate for absorptive encapsulation and controlled release of protein therapeutics. Biomaterials **31,** 9040, 2010.
8. Hollister, S.J. Porous scaffold design for tissue engineering. Nat Mater **4,** 518, 2005.
9. Peppas, N.A., Hilt, J.Z., Khademhosseini, A., and Langer, R. Hydrogels in biology and medicine: from molecular principles to bionanotechnology. Adv Mater **18,** 1345, 2006.
10. Khademhosseini, A., and Langer, R. Microengineered hydrogels for tissue engineering. Biomaterials **28,** 5087, 2007.
11. Nichol, J.W., and Khademhosseini, A. Modular tissue engineering: engineering biological tissues from the bottom up. Soft Matter **5,** 1312, 2009.
12. Rouwkema, J., Rivron, N.C., and van Blitterswijk, C.A. Vascularization in tissue engineering. Trends Biotechnol **26,** 434, 2008.
13. McGuigan, A.P., and Sefton, M.V. Vascularized organoid engineered by modular assembly enables blood perfusion. Proc Natl Acad Sci U S A **103,** 11461, 2006.
14. Reneker, D.H., and Chun, I. Nanometre diameter fibres of polymer, produced by electrospinning. Nanotechnology **7,** 216, 1996.
15. Yoshimoto, H., Shin, Y.M., Terai, H., and Vacanti, J.P. A biodegradable nanofiber scaffold by electrospinning and its potential for bone tissue engineering. Biomaterials **24,** 2077, 2003.
16. Xiao, J., Duan, H., Liu, Z., Wu, Z., Lan, Y., Zhang, W., *et al.* Construction of the recellularized corneal stroma using porous acellular corneal scaffold. Biomaterials **32,** 6962, 2011.
17. Choi, S.W., Yeh, Y.C., Zhang, Y., Sung, H.W., and Xia, Y. Uniform beads with controllable pore sizes for biomedical applications. Small **6,** 1492, 2010.
18. Salerno, A., Guarnieri, D., Iannone, M., Zeppetelli, S., and Netti, P.A. Effect of micro- and macroporosity of bone tissue three-dimensional-poly(epsilon-caprolactone) scaffold on human mesenchymal stem cells invasion, proliferation, and differentiation *in vitro*. Tissue Eng Part A **16,** 2661, 2010.
19. Fozdar, D.Y., Soman, P., Lee, J.W., Han, L.H., and Chen, S. Three-dimensional polymer constructs exhibiting a tunable negative Poisson's ratio. Adv Funct Mater **21,** 2712, 2011.
20. Ovsianikov, A., Schlie, S., Ngezahayo, A., Haverich, A., and Chichkov, B.N. Two-photon polymerization technique for microfabrication of CAD-designed 3D scaffolds from commercially available photosensitive materials. J Tissue Eng Regen Med **1,** 443, 2007.
21. Arcaute, K., Mann, B.K., and Wicker, R.B. Stereolithography of three-dimensional bioactive poly(ethylene glycol) constructs with encapsulated cells. Ann Biomed Eng **34,** 1429, 2006.
22. Tsang, V.L., and Bhatia, S.N. Three-dimensional tissue fabrication. Adv Drug Deliv Rev **56,** 1635, 2004.
23. Houchin-Ray, T., Swift, L.A., Jang, J.H., and Shea, L.D. Patterned PLG substrates for localized DNA delivery and directed neurite extension. Biomaterials **28,** 2603, 2007.
24. Hong, Y., Guan, J., Fujimoto, K.L., Hashizume, R., Pelinescu, A.L., and Wagner, W.R. Tailoring the degradation kinetics of poly(ester carbonate urethane)urea thermoplastic elastomers for tissue engineering scaffolds. Biomaterials **31,** 4249, 2010.
25. Chen, V.J., and Ma, P.X. Nano-fibrous poly(L-lactic acid) scaffolds with interconnected spherical macropores. Biomaterials **25,** 2065, 2004.
26. Hwang, C.M., Sant, S., Masaeli, M., Kachouie, N.N., Zamanian, B., Lee, S.H., *et al.* Fabrication of three-dimensional

porous cell-laden hydrogel for tissue engineering. Biofabrication **2,** 035003, 2010.
27. Scott, E.A., Nichols, M.D., Kuntz-Willits, R., and Elbert, D.L. Modular scaffolds assembled around living cells using poly(ethylene glycol) microspheres with macroporation via a non-cytotoxic porogen. Acta Biomater **6,** 29, 2010.
28. Niino, T., Hamajima, D., Montagne, K., Oizumi, S., Naruke, H., Huang, H., *et al.* Laser sintering fabrication of three-dimensional tissue engineering scaffolds with a flow channel network. Biofabrication **3,** 034104, 2011.
29. Suri, S., and Schmidt, C.E. Cell-laden hydrogel constructs of hyaluronic acid, collagen, and laminin for neural tissue engineering. Tissue Eng Part A **16,** 1703, 2010.
30. Chew, S.Y., Mi, R., Hoke, A., and Leong, K.W. Aligned protein-polymer composite fibers enhance nerve regeneration: a potential tissue-engineering platform. Adv Funct Mater **17,** 1288, 2007.
31. Miller, J.S., Stevens, K.R., Yang, M.T., Baker, B.M., Nguyen, D.H., Cohen, D.M., *et al.* Rapid casting of patterned vascular networks for perfusable engineered three-dimensional tissues. Nat Mater **11,** 768, 2012.
32. Radisic, M., Yang, L., Boublik, J., Cohen, R.J., Langer, R., Freed, L.E., *et al.* Medium perfusion enables engineering of compact and contractile cardiac tissue. Am J Physiol Heart Circ Physiol **286,** H507, 2004.
33. Chrobak, K.M., Potter, D.R., and Tien, J. Formation of perfused, functional microvascular tubes *in vitro*. Microvasc Res **71,** 185, 2006.
34. Lynam, D., Bednark, B., Peterson, C., Welker, D., Gao, M., and Sakamoto, J.S. Precision microchannel scaffolds for central and peripheral nervous system repair. J Mater Sci Mater Med **22,** 2119, 2011.
35. Nichol, J.W., Koshy, S.T., Bae, H., Hwang, C.M., Yamanlar, S., and Khademhosseini, A. Cell-laden microengineered gelatin methacrylate hydrogels. Biomaterials **31,** 5536, 2010.
36. Golden, A.P., and Tien, J. Fabrication of microfluidic hydrogels using molded gelatin as a sacrificial element. Lab Chip **7,** 720, 2007.
37. Ling, Y., Rubin, J., Deng, Y., Huang, C., Demirci, U., Karp, J.M., *et al.* A cell-laden microfluidic hydrogel. Lab Chip **7,** 756, 2007.
38. Choi, N.W., Cabodi, M., Held, B., Gleghorn, J.P., Bonassar, L.J., and Stroock, A.D. Microfluidic scaffolds for tissue engineering. Nat Mater **6,** 908, 2007.
39. Cuchiara, M.P., Allen, A.C., Chen, T.M., Miller, J.S., and West, J.L. Multilayer microfluidic PEGDA hydrogels. Biomaterials **31,** 5491, 2010.
40. Visconti, R.P., Kasyanov, V., Gentile, C., Zhang, J., Markwald, R.R., and Mironov, V. Towards organ printing: engineering an intra-organ branched vascular tree. Expert Opin Biol Ther **10,** 409, 2010.
41. Mondrinos, M.J., Dembzynski, R., Lu, L., Byrapogu, V.K., Wootton, D.M., Lelkes, P.I., *et al.* Porogen-based solid freeform fabrication of polycaprolactone-calcium phosphate scaffolds for tissue engineering. Biomaterials **27,** 4399, 2006.
42. Han, L.H., Lai, J.H., Yu, S., and Yang, F. Dynamic tissue engineering scaffolds with stimuli-responsive macroporosity formation. Biomaterials **34,** 4251, 2013.
43. Fairbanks, B.D., Schwartz, M.P., Bowman, C.N., and Anseth, K.S. Photoinitiated polymerization of PEG-diacrylate with lithium phenyl-2,4,6-trimethylbenzoylphosphinate: polymerization rate and cytocompatibility. Biomaterials **30,** 6702, 2009.
44. Shin, S.J., Park, J.Y., Lee, J.Y., Park, H., Park, Y.D., Lee, K.B., *et al.* "On the fly" continuous generation of alginate fibers using a microfluidic device. Langmuir **23,** 9104, 2007.
45. Graham, F.L., Smiley, J., Russell, W.C., and Nairn, R. Characteristics of a human cell line transformed by DNA from human adenovirus type 5. J Gen virol **36,** 59, 1977.
46. Bellan, L.M., Pearsall, M., Cropek, D.M., and Langer, R. A 3D interconnected microchannel network formed in gelatin by sacrificial shellac microfibers. Adv Mater **24,** 5187, 2012.
47. Anderson, S.B., Lin, C.C., Kuntzler, D.V., and Anseth, K.S. The performance of human mesenchymal stem cells encapsulated in cell-degradable polymer-peptide hydrogels. Biomaterials **32,** 3564, 2011.
48. Lutolf, M.P., Lauer-Fields, J.L., Schmoekel, H.G., Metters, A.T., Weber, F.E., Fields, G.B., *et al.* Synthetic matrix metalloproteinase-sensitive hydrogels for the conduction of tissue regeneration: engineering cell-invasion characteristics. Proc Natl Acad Sci U S A **100,** 5413, 2003.

Address correspondence to:
Fan Yang, PhD
Department of Bioengineering
Stanford University
300 Pasteur Drive
Edwards R105, MC5341
Stanford, CA 94305

E-mail: fanyang@stanford.edu

Received: March 17, 2013
Accepted: May 29, 2013
Online Publication Date: July 17, 2013